

Article

Sexual Dimorphic Rightward Lateralization of Cerebral Sulcal Infolding in Cynomolgus Monkeys (*Macaca fascicularis*)

Kazuhiko Sawada ^{1,*}  and Shigeyoshi Saito ^{2,3} 

¹ Department of Nutrition, Faculty of Medical and Health Sciences, Tsukuba International University, Tsuchiura 300-0051, Japan

² Department of Medical Physics and Engineering, Division of Health Sciences, Graduate School of Medicine, Osaka University, Osaka 565-0871, Japan

³ Department of Advanced Medical Technologies, National Cerebral and Cardiovascular Center Research Institute, Osaka 564-8565, Japan

* Correspondence: k-sawada@tius.ac.jp; Tel.: +81-29-883-6032

Abstract: Cerebral sulcal infolding exhibits unique species-related lateralization patterns. The present investigation aimed to characterize the asymmetric patterns of sulcal infolding in cynomolgus monkeys and their sexual dimorphism. Three-dimensional magnetic resonance (MR) images were acquired at 7-Tesla from the fixed brains of adult male ($n = 5$) and female ($n = 5$) monkeys. The gyrification index (GI) was estimated on MR images throughout the cerebral cortex (global-GI) or in the representative primary sulci (sulcal-GI). The global-GI did not differ between the sexes when the ipsilateral sides were compared. Although there was no sex difference in the sulcal-GI of the ipsilateral sides of any primary sulci, a significant right bias of the sulcal-GI was noted in the inferior rams of the arcuate sulcus and circular sulcus in males but not in females. Secondary sulcal emergence was examined to assess sulcal infolding asymmetry at the individual and population levels. Nonbiased asymmetric emergence was noted in the posterior supraprincipal dimple in both sexes and the rostral sulcus in females. Notably, the emergence of the superior postcentral dimple was significantly right-lateralized in females. The findings revealed right-biased sulcal infolding in male and female cynomolgus monkeys, although the lateralized cortical regions differed between the sexes.

Keywords: macaque; arcuate sulcus; circular sulcus; postcentral sulcus; sex difference; MRI



Citation: Sawada, K.; Saito, S. Sexual Dimorphic Rightward Lateralization of Cerebral Sulcal Infolding in Cynomolgus Monkeys (*Macaca fascicularis*). *Symmetry* **2023**, *15*, 1164. <https://doi.org/10.3390/sym15061164>

Academic Editors: John H. Graham and Chris Bishop

Received: 1 March 2023

Revised: 23 May 2023

Accepted: 24 May 2023

Published: 28 May 2023



Copyright: © 2023 by the authors. Licensee MDPI, Basel, Switzerland. This article is an open access article distributed under the terms and conditions of the Creative Commons Attribution (CC BY) license (<https://creativecommons.org/licenses/by/4.0/>).

1. Introduction

The cerebral cortex is convoluted to various degrees in many species of mammals [1]. In particular, the complexity of cortical convolution implicates asymmetry of sulcal infolding in higher-order primates, including humans, apes, and old-world monkeys [2]. Although cerebral sulci begin to emerge at midgestation in primates, sulcal morphology changes during postnatal maturation to form asymmetric patterns [3]. Several reports have documented the involvement of sulcal asymmetry in cerebral function in humans, including rightward asymmetry of the superior temporal sulcus and fMRI-defined right-lateralized voice-selective responses [4,5], leftward asymmetry of the central sulcus and right-handedness [6,7], and leftward asymmetry of the paracingulate sulcus and cognition [8,9].

Several approaches, such as the sulcal length, depth, and surface area, have been used to examine the asymmetry of sulcal infolding [10,11]. Our previous study using cynomolgus monkeys revealed that the arcuate sulcus length was right-lateralized in males but symmetrical in females when measuring the sulcal length by placing a cotton thread directly on the entire length of the cerebral sulci (the “cotton thread” method) [10]. However, this method does not provide any information other than sulcal length for evaluating sulcal infolding, that is, the sulcal surface areas and depths. The degree of infolding of specific cerebral sulci can be assessed using the sulcal-gyrification index (sulcal-GI) [12],

which is obtained by modifying the gyrification index that quantitatively assesses the convolution throughout the cerebral cortex designed originally by Zilles et al. (1988) [13]. The sulcal-GI fluctuates with changes in the morphology of specific sulci, that is, the length, depth, width, and surface areas. The sulcal-GI is further altered by cortical growth and is correlated highly with cortical expansion, particularly in primary sulci infolded in multimodal association cortices [12]. Here, we applied the sulcal-GI to comprehensively assess asymmetric patterns of cerebral sulcal infolding and characterize the asymmetry in cerebral surface morphology and its sexual dimorphism in adult cynomolgus monkeys using magnetic resonance imaging (MRI)-based morphometry.

2. Materials and Methods

2.1. Samples

This study used three-dimensional (3D) MR images, which were obtained from the fixed brains of sexually mature male ($n = 5$) and female ($n = 5$) cynomolgus monkeys (*Macaca fascicularis*) at 3.5–6.6 years of age [14]. These brain samples were used in our previous study [10], which was approved by the Institutional Animal Care and Use Committee of Shin Nippon Biomedical Laboratories (approval code: B999-178). The samples were fixed using intracardiac perfusion with 0.9% NaCl followed by 4% paraformaldehyde in 0.1 M phosphate buffer (pH 7.4) under deep anesthesia with an intravenous injection of sodium pentobarbital (26 mg/kg; Tokyo Chemical Industry, Tokyo, Japan) and immersed in the same fixative [10].

Ex vivo MRI scans were performed using a horizontal 7.0 T scanner (BioSpec 70/30 USR; Bruker Biospin, Ettlingen, Germany) with an 86 mm volume coil. A transmit/receive quadrature 86 mm volume coil was used for image acquisition. Samples were placed horizontally on an MRI cradle. First, localizer scans were used for the accurate positioning of the brain samples inside the magnet. The sample was positioned to have the center of the brainstem approximately located at the magnet's isocenter. This was used to acquire 3D short TR/TE (typical T_1 -weighted parameter setting) MR images covering the entire fixed brain using rapid acquisition with a relaxation enhancement (RARE) sequence and the following parameters: repetition time (TR) = 400 ms; echo time (TE) = 6 ms (effective TE = 19.2 ms); RARE factor = 4; field of view (FOV) = $72 \times 64 \times 47.5 \text{ mm}^3$; acquisition matrix = $288 \times 256 \times 192$; voxel size = $250 \times 250 \times 250 \mu\text{m}^3$; number of acquisitions (NEX) = 4; and total scan time = 5 h, 27 min, and 36 s. Short TR/TE images were directly reconstructed at the scan workstation by using Paravision 7.0 (Bruker Biospin, Ettlingen, Germany) and subsequently imported to SliceOmatic software version 4.3 (TomoVision, Montreal, QC, Canada) for visualization and processing.

2.2. MRI-Based Morphometry

All 3D MR images were used to measure the fronto-occipital (FO) length, volume, and surface area of the cerebral cortex and to calculate the global-gyrification index (global-GI) and sulcal-GI. According to our previous study [12], the cortical gray matter of the left and right cerebral hemispheres was segmented semiautomatically on MR images at the coronal (axial) plane using the "Morpho" tool of the SliceOmatic software version 4.3 (TomoVision, Montreal, QC, Canada) based on image contrast. The FO length (length of the cerebral cortex from the frontal pole through the occipital pole) was measured on 3D-rendered images, which were reconstructed based on the segmented images using the 3D-rendering module of the same software. The volume (mm^3) was calculated by multiplying the sum of the segmented areas by the slice thickness ($250 \mu\text{m}$). The cortical surface area in the sulcal grooves was computed from 3D MR images using SliceOmatic software 4.3 (TomoVision). The surface areas of the 26 primary sulci, shown in Figure 1 and Figure S1, were also calculated. Furthermore, the cerebral sulci not involved in gyral demarcations were defined as secondary sulci (see Figure S1). The surface areas of the 12 secondary sulci were then summed up.

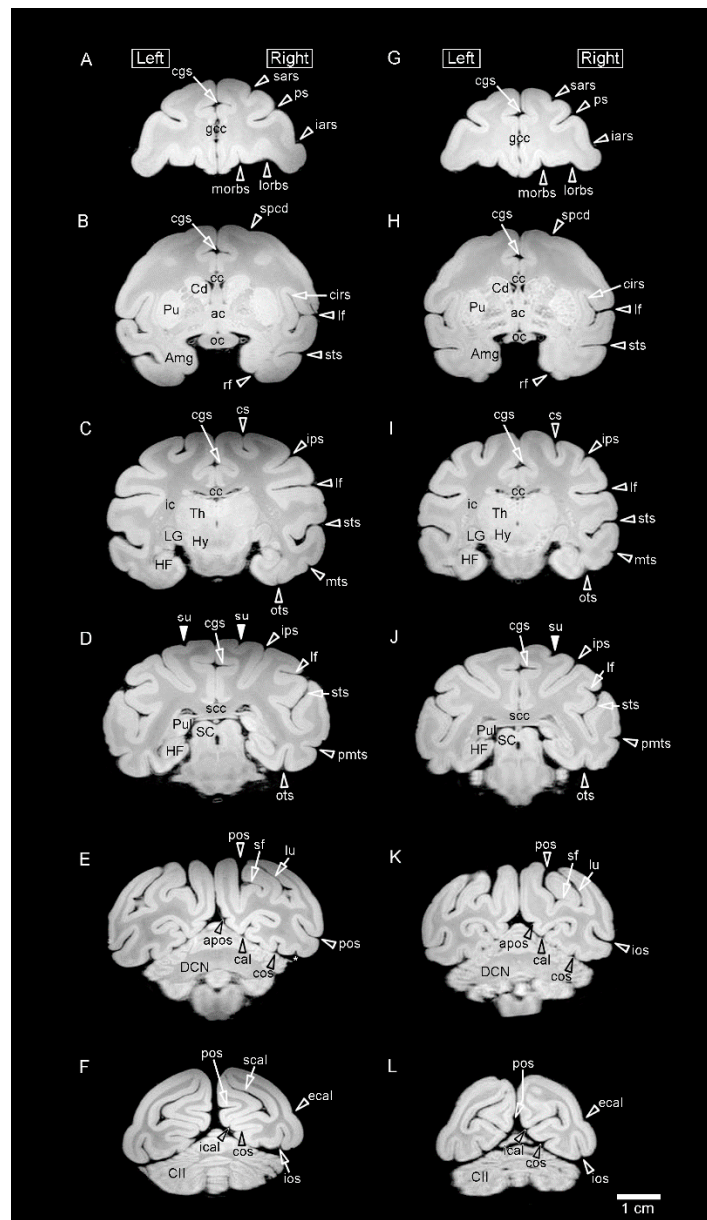


Figure 1. Representative coronal (axial) MR images (using a RARE sequence with a short TR and the minimum TE settings) obtained from fixed brains of sexually mature cynomolgus monkeys. (A–F) Coronal MR images of the male brain at rostral to caudal levels. (G–L) Coronal MR images of the female brain at rostral to caudal levels. MR images on the same lines are identical levels seen at: (A,G) the rostral end of the genu of corpus callosum (gcc); (B,H) the anterior commissure; (C,I) the lateral geniculate nucleus (LG) of the thalamus; (D,J) the splenium of corpus callosum (scc); (E,K) the deep cerebellar nucleus (DCN); and (F,L) the crus II of ansiform lobule (CII) of cerebellum. Amg, amygdala; apos, anterior parietooccipital sulcus; cal, calcarine sulcus; cgs, cingulate sulcus; cc, corpus callosum; Cd, caudate nucleus; cirs, circular sulcus; cos, collateral sulcus; cs, central sulcus; ecal, external calcarine sulcus; HF, hippocampal formation; Hy, hypothalamus; iars, inferior ram of arcuate sulcus; ic, internal capsule; ical, inferior calcarine sulcus; ios, inferior occipital sulcus; ips, intraparietal sulcus; lf, lateral fissure; lorbs, lateral orbital sulcus; lu, lunate sulcus; morb, medial orbital sulcus; mts, middle temporal sulcus; oc, optic chiasma; ots, occipitotemporal sulcus; pmts, posterior middle temporal sulcus; pos, parietooccipital sulcus; ps, principal sulcus; Pu, putamen; Pul, pulvinar of the thalamus; rf, rhinal fissure; sars, superior ram of arcuate sulcus; SC, superior colliculus; scal, superior calcarine sulcus; sf, simian fossa; spcd, superior precentral dimple; sts, superior temporal sulcus; su, superior postcentral dimple; Th, thalamus.

The degree of sulcal infolding was estimated throughout the cerebral cortex (global-GI) or in 26 primary sulci (Figure S1) (sulcal-GI) according to our previous procedure [12]. The global-GI and sulcal-GI were calculated using all MR images in the coronal plane by the proportion of the outer contours of the cerebral cortex to the sum of the sulcal perimeters and the proportion to the perimeters of the specific primary sulci, respectively. Furthermore, the sulcal-GIs of the 12 secondary sulci (Figure S1) were calculated and summed.

2.3. Asymmetric-Quotient Analysis

The asymmetry quotient (AQ) was estimated using the formula $((R - L) / \{(R + L) \times 0.5\})$ to assess the leftward or rightward bias of the cortical volume, FO length, cortical surface area, global-GI, and all sulcal-GI examined. The direction of asymmetry was indicated by AQ values: positive value = rightward bias and negative value = leftward bias [15].

2.4. Incidence of Secondary Sulci

The incidence of secondary sulci was separately calculated for the left and right cerebral hemispheres. Furthermore, the percentage of individuals with secondary sulci appearing on either the left or the right side was calculated to assess the asymmetric emergence of secondary sulci at the individual level.

2.5. Statistical Analysis

The left/right-side differences in the cortical volumes, cortical surface area, FO length of the cerebral hemispheres, and global-GI were compared using a paired sample *t*-test. Sex differences in these four measurements were statistically evaluated using a one-way analysis of variance (ANOVA), followed by a two-tailed Student's *t*-test. We further evaluated the left/right side differences in the sulcal surface areas and sulcal-GIs of the 26 primary sulci and the summed values of the surface areas and sulcal-GIs of the secondary sulci using a paired sample *t*-test. Sex-associated changes in the ipsilateral sides of these sulcal-GIs were assessed using a repeated measures three-way ANOVA with sex as an intergroup factor and the cerebral sulci as an intragroup factor. Sexual differences were assessed on the ipsilateral side of each measurement using Scheffé's test for post hoc testing, following simple main effects at $p < 0.05$. The AQ values of the sulcal surface areas and sulcal-GIs were analyzed using a one-sample *t*-test to determine any significant population-level asymmetry.

The incidence of secondary sulci on the left and right sides of the cerebral cortex was estimated using the chi-square test, and the percentage of individuals with secondary sulci appearing on either the left or the right side was evaluated using a one-sample *t*-test.

3. Results

3.1. MR Images and 3D-Rendered Images

Representative MR images of the brain from sexually mature male and female cynomolgus monkeys in the coronal plane are shown in Figure 1. An ex vivo high-field MRI using a RARE sequence with a short TR and minimum TE settings (T_1W parameter setting) reduced the signal contrast in the white matter of the fixed brain in the paraformaldehyde solution. We further reconstructed the cerebral-cortical surface morphology by 3D-rendered images calculated using MR images (Figure 2). Both the MR and 3D-rendered images could distinguish the primary and secondary sulci (Figures 1 and 2) that had been observed in gross anatomical examinations.

differences were observed with a significantly greater FO length in males than in females but not in the cortical volume, cortical surface area, and global-GI (Table 1).

Table 1. Left and right sides of the cortical volume, cortical surface area, fronto-occipital (FO) length of the cerebral hemispheres, global-gyrification index (global-GI), and asymmetry quotient (AQ) values of these four measurements in adult cynomolgus monkeys.

	Male (n = 5)			Female (n = 5)		
	Left	Right	AQ Values	Left	Right	AQ Values
Volume (mm ³)	12,847 ± 1347	12,740 ± 1178	−0.007 ± 0.014	11,626 ± 902	11,688 ± 878	0.005 ± 0.021
Surface area (mm ²)	6661 ± 587	6613 ± 542	−0.007 ± 0.008	7287 ± 457	7252 ± 381	−0.004 ± 0.023
FO length (mm)	60.8 ± 2.2 ^a	60.7 ± 2.3 ^b	−0.002 ± 0.006	49.6 ± 1.6	49.7 ± 1.2	0.002 ± 0.010
Global-GI	1.683 ± 0.054	1.688 ± 0.814	0.003 ± 0.008	1.684 ± 0.013	1.683 ± 0.02	0.000 ± 0.005

Mean ± Standard deviation. ^a $p = 0.000012$, ^b $p = 0.000003$ vs. ipsilateral side of females (Student's *t*-test).

The surface areas were significantly right-lateralized in the circular sulcus and in the medial orbital sulcus in males. There was no left/right-side bias in the surface areas of the other primary sulci examined in males (Table 2). In contrast, the summed surface areas of the secondary sulci were significantly right-lateralized in females, although no primary sulci exhibited significant left/right-side differences in their surface areas (Table 2). A significant population level of asymmetry in the sulcal surface areas was revealed to be leftward in the medial orbital sulcus of males and rightward in the circular sulcus of males and the secondary sulci of females by AQ analysis with a one-sample *t*-test (Table 3). When comparing the ipsilateral sides of the sulcal surface areas between sexes, there was no sex difference in any primary sulci examined (Table 2). The summed areas of the secondary sulci did not differ between males and females (Table 2).

Table 2. Sulcal surface areas of the left and right sides of the cerebral cortex in adult cynomolgus monkeys.

	Male (n = 5)		Female (n = 5)	
	Left	Right	Left	Right
Major cerebral sulci				
Lateral fissure (lf)	353.1 ± 56.9	352.3 ± 54.0	386.2 ± 50.9	386.6 ± 50.4
Central sulcus (cs)	166.9 ± 34.6	162.6 ± 26.5	168.0 ± 26.2	168.3 ± 13.0
Parietooccipital sulcus (pos)	73.7 ± 22.9	64.5 ± 34.0	100.2 ± 26.7	101.0 ± 13.3
Calcarine sulcus (cal)	323.7 ± 41.0	307.5 ± 31.2	319.4 ± 33.4	309.4 ± 31.4
Cingulate sulcus (cgs)	264.0 ± 30.8	257.1 ± 28.6	301.9 ± 35.7	303.6 ± 42.2
Circular sulcus (cirs)	229.5 ± 38.5	239.9 ± 35.9	238.1 ± 33.8	240.6 ± 35.8
Frontal lobe				
Arcuate sulcus, superior ram (sars)	65.3 ± 16.9	65.2 ± 14.3	67.8 ± 14.5	71.9 ± 12.6
Arcuate sulcus, inferior ram (iars)	73.8 ± 18.7	74.8 ± 17.2	86.8 ± 20.6	85.4 ± 14.7
Principal sulcus (ps)	166.1 ± 17.8	167.4 ± 31.8	188.3 ± 28.2	185.5 ± 25.0
Medial orbital sulcus (morb)	99.2 ± 19.9	94.7 ± 20.9	132.8 ± 21.6	129.8 ± 18.7
Lateral orbital sulcus (lorb)	42.4 ± 21.7	43.1 ± 13.6	72.2 ± 10.8	63.6 ± 23.4
Olfactory sulcus (olf)	5.4 ± 0.8	6.2 ± 1.3	10.1 ± 8.9	10.4 ± 9.5
Parietal lobe				
Intraparietal sulcus (ips)	335.6 ± 59.5	317.9 ± 51.3	335.1 ± 24.5	327.6 ± 20.3
Temporal lobe				
Superior temporal sulcus (sts)	472.3 ± 109.2	474.7 ± 97.1	542.3 ± 36.9	540.2 ± 43.3
Occipitotemporal sulcus (ots)	130.2 ± 73.3	134.6 ± 43.0	146.2 ± 26.8	140.7 ± 15.8
Anterior middle temporal sulcus (amts)	59.7 ± 23.1	55.2 ± 11.0	58.8 ± 8.0	52.5 ± 13.0
Posterior middle temporal sulcus (pmts)	25.2 ± 9.7	37.4 ± 20.96	45.5 ± 12.7	38.1 ± 17.2
Rhinal fissure (rf)	22.3 ± 7.4	24.1 ± 7.9	16.0 ± 6.9	17.2 ± 8.9
Collateral sulcus (cos)	77.7 ± 26.2	71.0 ± 18.5	92.1 ± 31.4	80.0 ± 14.9

Table 2. Cont.

	Male (n = 5)		Female (n = 5)	
	Left	Right	Left	Right
Occipital lobe				
Lunate sulcus (lu)	101.8 ± 19.0	102.7 ± 5.2	113.7 ± 23.3	109.0 ± 15.5
Inferior occipital sulcus (ios)	175.9 ± 45.8	183.0 ± 25.2	220.9 ± 28.8	225.1 ± 10.1
External calcarine sulcus (ecal)	33.1 ± 6.7	27.6 ± 8.7	47.9 ± 13.3	50.6 ± 17.0
Superior calcarine sulcus (scal)	75.6 ± 10.3	64.2 ± 15.2	91.1 ± 39.3	84.8 ± 32.4
Inferior calcarine sulcus (ical)	75.7 ± 27.2	78.7 ± 26.2	79.7 ± 32.5	84.6 ± 31.5
Simian fossa (sf)	136.2 ± 18.0	121.4 ± 21.9	121.4 ± 21.9	117.2 ± 27.6
Limbic cortex/Others				
Anterior parietooccipital sulcus (apos)	44.7 ± 21.4	44.7 ± 13.6	24.5 ± 20.2	26.6 ± 17.2
Secondary sulci	195.5 ± 51.1	188.2 ± 67.4	139.5 ± 41.3	170.5 ± 49.2

Mean ± Standard deviation. Gray column in the cirs: $p = 0.020926$, Gray column in the morb: $p = 0.011398$, Gray column in secondary sulci: $p = 0.039351$, left vs. right side (paired sample t -test).

Table 3. Asymmetry quotient (AQ) of the sulcal surface areas of the cerebral cortex in adult cynomolgus monkeys.

	AQ Values	
	Male (n = 5)	Female (n = 5)
Major cerebral sulci		
Lateral fissure (lf)	−0.001 ± 0.039	0.001 ± 0.050
Central sulcus (cs)	−0.019 ± 0.072	0.010 ± 0.099
Parietooccipital sulcus (pos)	−0.202 ± 0.219	0.029 ± 0.141
Calcarine sulcus (cal)	−0.049 ± 0.037	−0.032 ± 0.085
Cingulate sulcus (cgs)	−0.026 ± 0.030	0.003 ± 0.041
Circular sulcus (cirs)	0.047 ± 0.034	0.010 ± 0.018
Frontal lobe		
Arcuate sulcus, superior ram (sars)	0.006 ± 0.156	0.065 ± 0.084
Arcuate sulcus, inferior ram (iars)	0.018 ± 0.029	−0.005 ± 0.160
Principal sulcus (ps)	−0.002 ± 0.110	−0.012 ± 0.042
Medial orbital sulcus (morb)	−0.050 ± 0.029	−0.019 ± 0.085
Lateral orbital sulcus (lorb)	0.067 ± 0.297	−0.179 ± 0.467
Olfactory sulcus (olf)	0.126 ± 0.208	0.006 ± 0.120
Parietal lobe		
Intraparietal sulcus (ips)	−0.052 ± 0.045	−0.022 ± 0.045
Temporal lobe		
Superior temporal sulcus (sts)	0.011 ± 0.048	−0.005 ± 0.031
Occipitotemporal sulcus (ots)	0.095 ± 0.196	−0.029 ± 0.163
Anterior middle temporal sulcus (amts)	−0.007 ± 0.320	−0.130 ± 0.296
Posterior middle temporal sulcus (pmts)	0.295 ± 0.522	−0.238 ± 0.235
Rhinal fissure (rf)	0.086 ± 0.109	0.041 ± 0.170
Collateral sulcus (cos)	−0.071 ± 0.093	−0.115 ± 0.235
Occipital lobe		
Lunate sulcus (lu)	0.020 ± 0.168	−0.031 ± 0.160
Inferior occipital sulcus (ios)	0.060 ± 0.164	0.024 ± 0.107
External calcarine sulcus (ecal)	−0.196 ± 0.330	0.046 ± 0.223
Superior calcarine sulcus (scal)	−0.177 ± 0.232	−0.061 ± 0.152
Inferior calcarine sulcus (ical)	0.051 ± 0.113	0.087 ± 0.176
Simian fossa (sf)	−0.069 ± 0.091	−0.048 ± 0.133
Limbic cortex/Others		
Anterior parietooccipital sulcus (apos)	0.064 ± 0.258	0.184 ± 0.643
Secondary sulci	−0.072 ± 0.311	0.197 ± 0.132

Mean ± Standard deviation. Gray column in the cirs: $p = 0.037513$, Gray column in the morb: $p = 0.017547$, Gray column in secondary sulci: $p = 0.028982$ significant left or right-sided bias (one-sample t -test).

The sulcal-GIs were significantly right-lateralized in the circular sulcus and inferior ram of the arcuate sulcus in males. There was no left/right-side bias of the sulcal-GIs of

other primary sulci and the summed GI of secondary sulci in males, even in the medial orbital sulcus, where the surface area was significantly left-lateralized (Table 4). In females, there was no left/right-side bias of the sulcal-GI of any primary sulci or the summed GI of secondary sulci (Table 4). AQ analysis with a one-sample *t*-test also indicated a population level of rightward asymmetry in the circular sulcus and inferior ram of the arcuate sulcus in males but not in females (Table 5). In addition, sex differences were not observed when comparing the ipsilateral sides of the sulcal-GIs and the summed GI of the secondary sulci (Table 4).

Table 4. Sulcal-gyrification index (sulcal-GI) of the left and right sides of the cerebral cortex in adult cynomolgus monkeys.

	Male (<i>n</i> = 5)		Female (<i>n</i> = 5)	
	Left	Right	Left	Right
Major cerebral sulci				
Lateral fissure (lf)	1.0577 ± 0.0084	1.0580 ± 0.0086	1.0619 ± 0.0074	1.0612 ± 0.0064
Central sulcus (cs)	1.0264 ± 0.0046	1.0260 ± 0.0045	1.0243 ± 0.0048	1.0245 ± 0.0028
Parietooccipital sulcus (pos)	1.0147 ± 0.0056	1.0130 ± 0.0077	1.0183 ± 0.0054	1.0186 ± 0.0031
Calcarine sulcus (cal)	1.0707 ± 0.0053	1.0688 ± 0.0032	1.0654 ± 0.0039	1.0635 ± 0.0039
Cingulate sulcus (cgs)	1.0522 ± 0.0046	1.0513 ± 0.0056	1.0535 ± 0.0055	1.0538 ± 0.0071
Circular sulcus (cirs)	1.0520 ± 0.0069	1.0546 ± 0.0054	1.0501 ± 0.0055	1.0506 ± 0.0056 ^a
Frontal lobe				
Arcuate sulcus, superior ram (sars)	1.0095 ± 0.0026	1.0106 ± 0.0028	1.0078 ± 0.0023	1.0083 ± 0.0020
Arcuate sulcus, inferior ram (iars)	1.0102 ± 0.0017	1.0113 ± 0.0017	1.0097 ± 0.0017	1.0102 ± 0.0013
Principal sulcus (ps)	1.0429 ± 0.0035	1.0449 ± 0.0048	1.0420 ± 0.0033	1.0421 ± 0.0037
Medial orbital sulcus (morb)	1.0121 ± 0.0030	1.0117 ± 0.0032	1.0119 ± 0.0020	1.0125 ± 0.0019
Lateral orbital sulcus (lorb)	1.0022 ± 0.0023	1.0018 ± 0.0007	1.0040 ± 0.0014	1.0042 ± 0.0038
Olfactory sulcus (olf)	1.0005 ± 0.0001	1.0006 ± 0.0002	1.0005 ± 0.0004	1.0006 ± 0.0005
Parietal lobe				
Intraparietal sulcus (ips)	1.0583 ± 0.0121	1.0580 ± 0.0109	1.0534 ± 0.0039	1.0528 ± 0.0030
Temporal lobe				
Superior temporal sulcus (sts)	1.0831 ± 0.0202	1.0837 ± 0.0180	1.0904 ± 0.0089	1.0897 ± 0.0089
Occipitotemporal sulcus (ots)	1.0182 ± 0.0156	1.0171 ± 0.0095	1.0173 ± 0.0035	1.0171 ± 0.0015
Anterior middle temporal sulcus (amts)	1.0052 ± 0.0022	1.0047 ± 0.0011	1.0048 ± 0.0012	1.0049 ± 0.0014
Posterior middle temporal sulcus (pmts)	1.0019 ± 0.0010	1.0034 ± 0.0025	1.0038 ± 0.0017	1.0031 ± 0.0027
Rhinal fissure (rf)	1.0022 ± 0.0007	1.0026 ± 0.0009	1.0010 ± 0.0006	1.0013 ± 0.0008
Collateral sulcus (cos)	1.0147 ± 0.0041	1.0142 ± 0.0031	1.0151 ± 0.0062	1.0133 ± 0.0025
Occipital lobe				
Lunate sulcus (lu)	1.0204 ± 0.0022	1.0217 ± 0.0007	1.0209 ± 0.0055	1.0204 ± 0.0033
Inferior occipital sulcus (ios)	1.0345 ± 0.0087	1.0371 ± 0.0049	1.0423 ± 0.0068	1.0435 ± 0.0058
External calcarine sulcus (ecal)	1.0007 ± 0.0005	1.0008 ± 0.0007	1.0019 ± 0.0020	1.0039 ± 0.0055
Superior calcarine sulcus (scal)	1.0213 ± 0.0062	1.0174 ± 0.0067	1.0223 ± 0.0092	1.0211 ± 0.0087
Inferior calcarine sulcus (ical)	1.0206 ± 0.0052	1.0214 ± 0.0051	1.0206 ± 0.0089	1.0221 ± 0.0074
Simian fossa (sf)	1.0327 ± 0.0023	1.0266 ± 0.0040	1.0266 ± 0.0040	1.0256 ± 0.0053
Limbic cortex/Others				
Anterior parietooccipital sulcus (apos)	1.0064 ± 0.0033	1.0069 ± 0.0024	1.0033 ± 0.0032	1.0037 ± 0.0029
Secondary sulci	1.0110 ± 0.0017	1.0127 ± 0.0017	1.0092 ± 0.0030	1.0084 ± 0.0026

Mean ± Standard deviation. Gray column in the cirs: $p = 0.008343$, Gray column in the iars: $p = 0.048349$, left vs. right sides (paired sample *t*-test).

3.3. Incidence of Secondary Sulci

Small or shallow indentations on the cerebral surface that were not involved in gyral demarcations were defined as secondary sulci. Their emergence varied not only among individuals but also between the left/right hemispheres within individuals (Table 6). Significantly asymmetrical emergences were marked in the posterior supraprincipal dimple in both sexes and the rostral sulcus and superior postcentral dimple only in females (Table 6). Although the incidence of the rostral sulcus and superior postcentral dimple was high (80%) in males, their emergence was symmetrical (Table 6). The emergence of the posterior

supraprincipal dimple and rostral sulcus was not biased toward either the left or right side. Notably, the superior postcentral dimple emerged significantly on the right side in females (Table 6).

Table 5. Asymmetry quotient (AQ) of the sulcal-gyrification index (sulcal-GI) of the cerebral cortex in adult cynomolgus monkeys.

	AQ Values	
	Male (<i>n</i> = 5)	Female (<i>n</i> = 5)
Major cerebral sulci		
Lateral fissure (lf)	0.000 ± 0.002	−0.001 ± 0.003
Central sulcus (cs)	0.000 ± 0.002	0.000 ± 0.002
Parietooccipital sulcus (pos)	−0.002 ± 0.002	0.000 ± 0.003
Calcarine sulcus (cal)	−0.002 ± 0.003	−0.002 ± 0.002
Cingulate sulcus (cgs)	−0.001 ± 0.002	0.000 ± 0.002
Circular sulcus (cirs)	0.003 ± 0.002	0.001 ± 0.002
Frontal lobe		
Arcuate sulcus, superior ram (sars)	0.001 ± 0.002	0.001 ± 0.001
Arcuate sulcus, inferior ram (iars)	0.001 ± 0.000	0.000 ± 0.001
Principal sulcus (ps)	0.002 ± 0.003	0.000 ± 0.003
Medial orbital sulcus (morb)	0.000 ± 0.001	0.001 ± 0.001
Lateral orbital sulcus (lorb)	0.000 ± 0.002	0.000 ± 0.003
Olfactory sulcus (olf)	0.000 ± 0.000	0.000 ± 0.002
Parietal lobe		
Intraparietal sulcus (ips)	0.000 ± 0.002	−0.001 ± 0.003
Temporal lobe		
Superior temporal sulcus (sts)	0.001 ± 0.004	−0.001 ± 0.003
Occipitotemporal sulcus (ots)	−0.001 ± 0.006	0.000 ± 0.003
Anterior middle temporal sulcus (amts)	−0.001 ± 0.001	0.000 ± 0.001
Posterior middle temporal sulcus (pmts)	0.001 ± 0.002	−0.001 ± 0.001
Rhinal fissure (rf)	0.000 ± 0.000	0.000 ± 0.000
Collateral sulcus (cos)	0.000 ± 0.001	−0.002 ± 0.005
Occipital lobe		
Lunate sulcus (lu)	0.001 ± 0.002	0.000 ± 0.004
Inferior occipital sulcus (ios)	0.003 ± 0.004	0.001 ± 0.004
External calcarine sulcus (ecal)	0.000 ± 0.000	0.002 ± 0.004
Superior calcarine sulcus (scal)	−0.004 ± 0.004	−0.001 ± 0.003
Inferior calcarine sulcus (ical)	0.001 ± 0.002	0.001 ± 0.003
Simian fossa (sf)	−0.001 ± 0.003	−0.001 ± 0.003
Limbic cortex/Others		
Anterior parietooccipital sulcus (apos)	0.001 ± 0.001	0.000 ± 0.001
Secondary sulci	0.002 ± 0.003	−0.001 ± 0.003

Mean ± Standard deviation. Gray column in the cirs: $p = 0.049024$, Gray column in the iars: $p = 0.008315$, Significant left- or right-side bias (One-sample *t*-test).

Table 6. Incidence of secondary sulci on the left and right sides of the cerebral cortex in adult cynomolgus monkeys.

	Male (<i>n</i> = 5)			Female (<i>n</i> = 5)		
	Left	Right	Asymmetrical	Left	Right	Asymmetrical
Frontal lobe						
Supr of arcuate sulcus (sas)	100% (5/5)	100% (5/5)	0% (0/5)	100% (5/5)	100% (5/5)	0% (0/5)
Anterior supraprincipal dimple (aspd)	80% (4/5)	100% (5/5)	20% (1/5)	0% (0/5)	40% (2/5)	0% (0/5)
Posterior supraprincipal dimple(pspd)	40% (2/5)	60% (3/5)	60% (3/5)	80% (4/5)	60% (3/5)	60% (3/5)
Superior precentral dimple (spcd)	100% (5/5)	100% (5/5)	0% (0/5)	100% (5/5)	80% (4/5)	20% (1/5)
Infraprincipal dimple (ipd)	80% (4/5)	60% (3/5)	40% (2/5)	80% (4/5)	40% (2/5)	0% (0/5)

Table 6. Cont.

	Male (n = 5)			Female (n = 5)		
	Left	Right	Asymmetrical	Left	Right	Asymmetrical
Anterior subcentral dimple (asd)	100% (5/5)	100% (5/5)	0% (0/5)	100% (5/5)	80% (4/5)	20% (1/5)
Intermediate orbital sulcus (iorb)	80% (4/5)	80% (4/5)	40% (2/5)	40% (2/5)	80% (4/5)	40% (2/5)
Rostral sulcus (ros)	80% (4/5)	80% (4/5)	0% (0/5) ^a	60% (3/5)	40% (2/5)	60% (3/5) ^a
Parietal lobe						
Superior postcentral dimple (su)	80% (4/5)	80% (4/5)	0% (0/5) ^a	20% (1/5)	80% (4/5)	60% (3/5) ^a
Posterior subcentral sulcus (pscs)	40% (2/5)	80% (4/5)	40% (2/5)	40% (2/5)	20% (1/5)	20% (1/5)
Temporal Lobe						
Intermediate middle temporal sulcus (imt)	80% (4/5)	60% (3/5)	20% (1/5)	80% (4/5)	80% (4/5)	40% (2/5)
Limbic cortex						
Subparietal sulcus (sbps)	60% (3/5)	60% (3/5)	0% (0/5)	40% (2/5)	60% (3/5)	20% (1/5)

The percentage of individuals with secondary sulci appearing on either the left or right side is expressed as “Asymmetrical”. The number of emerging secondary sulci on each side is shown in parentheses. ^a: $p = 0.05$ male vs. female (Chi-square test); Gray column: $p = 0.05$ left vs. right sides (one-sample t -test); Light gray column: $p = 0.05$ significant secondary sulci emerging asymmetrically (one-sample t -test).

4. Discussion

The present study revisited sulcal infolding asymmetry in the cerebral cortex of male and female cynomolgus monkeys using MRI-based morphometry. Our previous study revealed rightward lateralization of the length of the arcuate sulcus in males but not in females [10]. In the present study, the inferior ram of the arcuate sulcus was significantly right-lateralized only in males at the population level. The consistent results between our previous and present studies suggest that the sulcal length largely reflects the asymmetry of arcuate sulcus infolding in male cynomolgus monkeys. The rightward asymmetry of the arcuate sulcus length was distinct in male cynomolgus monkeys from adolescence to adulthood, following the completion of primary sulcogenesis [3]. The frontal lobe contained significantly greater levels of androgen receptors on the right side than on the left side in male rhesus monkeys, but this was inconsistent between the left and right sides in females [16]. Arcuate sulcus infolding may lateralize rightward under the influence of androgens in male cynomolgus monkeys.

The inferior ram of the arcuate sulcus in macaques is anatomically identical to the precentral sulcus in humans and the superior precentral sulcus in captive chimpanzees (*Pan troglodytes*) [1], which forms the posterior boundary of the dorsolateral and ventrolateral prefrontal cortex (dlPFC and vlPFC) [17]. The frontoparietal network, including the dlPFC, has functional connections associated with cognitive control to the contralateral sides of crus II of the ansiform lobule of the cerebellar hemisphere [18]. Contralateral functional connections between the cerebral association cortices and cerebellar hemispheres are known to implicate the complementary lateralized development of these two brain regions [19]. Therefore, right-lateralized infolding of the inferior ram of the arcuate sulcus in male cynomolgus monkeys may be involved in the significant leftward volume laterality of crus II obtained using the same MRI data in our previous study [14].

The present study further revealed a significant right-lateralized infolding of the circular sulcus in male, but not female, cynomolgus monkeys, which had not been demonstrated in our previous study that used the “cotton thread” method [10]. The insular cortex is depicted by the circular sulcus, and the right side of the anterior part is included in the temporoparietal junction with salience-related brain networks, together with the right dlPFC [20]. Therefore, right-lateralized infolding of the circular sulcus in male cynomolgus monkeys may be linked with the ipsilateralized folding of the inferior ram of the arcuate sulcus.

On the other hand, population-level leftward asymmetry of the surface area, rather than the sulcal-GI, was observed in the medial orbital sulcus of male cynomolgus monkeys. However, it is difficult to speculate on the functional and evolutionary implications of the

left lateralization of this sulcus. The orbitofrontal cortex is convoluted with high variability in rhesus macaques and humans [21].

Another finding of the present study was the asymmetrical emergence of small or shallow indentations on the cerebral surface, defined as secondary sulci. The majority of the secondary sulci emerged asymmetrically, without left- or right-side biases. Nonbiased asymmetrical development was also found in the secondary sulci emerging on the cerebral cortex of common marmosets [2]. A notable finding of the present study was that the emergence of the superior postcentral dimple, identical to the postcentral sulcus in humans [1], was significantly right-lateralized in females but symmetrical in males. This dimple was observed in 80% of males bilaterally and in females on the right side, suggesting poor development of the left postcentral and supraparietal cortical regions in females. In addition, the central sulcus, superior temporal sulcus, and parietooccipital sulcus emerged as secondary sulci asymmetrically without left- or right-side biases in common marmosets [2]. These sulci are defined as the primary sulci after the split between new-world and old-world monkeys [2]. Therefore, the superior postcentral dimple in old-world monkeys may be infolded by the expansion of surrounding cortical regions in subsequent evolutionary processes and defined as the primary sulcus, named the “postcentral sulcus” after the split into higher-order primates such as apes and humans.

5. Conclusions

The present study quantitatively examined the asymmetrical development of cerebral sulcal infolding in cynomolgus monkeys using MRI-based morphometry and obtained consistent results with our previous study that measured the sulcal length on the cortical surface using the cotton-thread method [10]. On the other hand, no left/right-side bias development of primary sulcal infolding and/or cortical folding has been observed in carnivores [22]. These animals have been found to develop leftward torque asymmetry of the cerebellum [23,24], similar to cynomolgus monkeys [14]. The presence of contralateral cerebro-cerebellar connectivity, which is involved in the lateralized development of the cerebral cortex in primates, is unclear in carnivores [19]. The lateralized infolding of the primary sulci may result from the functional specification of the left/right cerebral hemispheres acquired in the course of primate evolution, with more remarkably developed characteristics compared to other mammalian species.

Supplementary Materials: The following supporting information can be downloaded at: <https://www.mdpi.com/article/10.3390/sym15061164/s1>, Figure S1: Sulcal maps of cynomolgus monkeys.

Author Contributions: Formal analysis, K.S.; Funding acquisition, S.S.; Methodology, K.S. and S.S.; Supervision, K.S.; Validation, K.S. and S.S.; Writing—original draft, K.S.; Writing—review & editing, K.S. and S.S. All authors have read and agreed to the published version of the manuscript.

Funding: This work was the result of using research equipment shared by the MEXT Project for promoting public utilization of advanced research infrastructure (program for supporting the construction of core facilities) (grant number JPMXS0450400021, JPMXS0450400022).

Data Availability Statement: Data available on request due to restrictions eg privacy or ethical. The data presented in this study are available on request from the corresponding author.

Conflicts of Interest: The authors declare no conflict of interest.

References

1. Zilles, K.; Palomero-Gallagher, N.; Amunts, K. Development of cortical folding during evolution and ontogeny. *Trends Neurosci.* **2013**, *36*, 275–284. [[CrossRef](#)] [[PubMed](#)]
2. Sawada, K. Cerebral sulcal asymmetry in macaque monkeys. *Symmetry* **2020**, *12*, 1509. [[CrossRef](#)]
3. Sakamoto, K.; Sawada, K.; Fukunishi, K.; Imai, N.; Sakata-Haga, H.; Fukui, Y. Postnatal change in sulcal length asymmetry in cerebrum of cynomolgus monkeys (*Macaca fascicularis*). *Anat. Rec. (Hoboken)* **2014**, *297*, 200–207. [[CrossRef](#)]
4. Bonte, M.; Frost, M.A.; Rutten, S.; Ley, A.; Formisano, E.; Goebel, R. Development from childhood to adulthood increases morphological and functional inter-individual variability in the right superior temporal cortex. *Neuroimage* **2013**, *83*, 739–750. [[CrossRef](#)] [[PubMed](#)]

5. Bodin, C.; Takerkart, S.; Belin, P.; Coulon, O. Anatomic-functional correspondence in the superior temporal sulcus. *Brain Struct. Funct.* **2018**, *223*, 221–232. [[CrossRef](#)] [[PubMed](#)]
6. Foundas, A.L.; Hong, K.; Leonard, C.M.; Heilman, K.M. Hand preference and magnetic resonance imaging asymmetries of the central sulcus. *Neuropsychiatry Neuropsychol. Behav. Neurol.* **1998**, *11*, 65–71.
7. Klöppel, S.; Mangin, J.F.; Vongersichten, A.; Frackowiak, R.S.; Siebner, H.R. Nurture versus nature: Long-term impact of forced right-handedness on structure of pericentral cortex and basal ganglia. *J. Neurosci.* **2010**, *30*, 3271–3275. [[CrossRef](#)] [[PubMed](#)]
8. Fornito, A.; Wood, S.J.; Whittle, S.; Fuller, J.; Adamson, C.; Saling, M.M.; Velakoulis, D.; Pantelis, C.; Yücel, M. Variability of the paracingulate sulcus and morphometry of the medial frontal cortex: Associations with cortical thickness, surface area, volume, and sulcal depth. *Hum. Brain Mapp.* **2008**, *29*, 222–236. [[CrossRef](#)]
9. Amiez, C.; Wilson, C.R.E.; Procyk, E. Variations of cingulate sulcal organization and link with cognitive performance. *Sci. Rep.* **2018**, *8*, 1–13. [[CrossRef](#)]
10. Imai, N.; Sawada, K.; Fukunishi, K.; Sakata-Haga, H.; Fukui, Y. Sexual dimorphism of sulcal length asymmetry in cerebrum of adult cynomolgus monkeys (*Macaca fascicularis*). *Congenit. Anom. (Kyoto)* **2011**, *51*, 161–166. [[CrossRef](#)]
11. Bogart, S.L.; Mangin, J.F.; Schapiro, S.J.; Reamer, L.; Bennett, A.J.; Pierre, P.J.; Hopkins, W.D. Cortical sulci asymmetries in chimpanzees and macaques: A new look at an old idea. *Neuroimage* **2012**, *61*, 533–541. [[CrossRef](#)] [[PubMed](#)]
12. Sawada, K.; Fukunishi, K.; Kashima, M.; Imai, N.; Saito, S.; Aoki, I.; Fukui, Y. Regional difference in sulcal infolding progression correlated with cerebral cortical expansion in cynomolgus monkey fetuses. *Congenit. Anom. (Kyoto)* **2017**, *57*, 114–117. [[CrossRef](#)]
13. Zilles, K.; Armstrong, E.; Schleicher, A.; Kretschmann, H.J. The human pattern of gyrification in the cerebral cortex. *Anat. Embryol.* **1988**, *179*, 173–179. [[CrossRef](#)]
14. Sawada, K.; Saito, S. Sex-related left-lateralized development of the crus II region of the ansiform lobule in cynomolgus monkeys. *Symmetry* **2022**, *14*, 1015. [[CrossRef](#)]
15. Hopkins, W.D.; Marino, L. Asymmetries in cerebral width in nonhuman primate brains as revealed by magnetic resonance imaging (MRI). *Neuropsychologia* **2000**, *38*, 493–499. [[CrossRef](#)] [[PubMed](#)]
16. Sholl, S.A.; Kim, K.L. Androgen receptors are differentially distributed between right and left cerebral hemispheres of the fetal male rhesus monkey. *Brain Res.* **1990**, *516*, 122–126. [[CrossRef](#)]
17. Miller, E.K.; Walls, J.D. The prefrontal cortex and executive brain functions. In *Fundamental Neuroscience*, 2nd ed.; Squire, L., Berg, D., Bloom, F.E., McConnell, S., Roberts, J.L., Spitzer, N.C., Zigmond, M.J., Eds.; Academic Press: San Diego, CA, USA, 2003; pp. 1353–1376.
18. Sang, L.; Qin, W.; Liu, Y.; Han, W.; Zhang, Y.; Jiang, T.; Yu, C. Resting-state functional connectivity of the vermal and hemi-spheric subregions of the cerebellum with both the cerebral cortical networks and subcortical structures. *Neuroimage* **2012**, *61*, 1213–1225. [[CrossRef](#)] [[PubMed](#)]
19. Wang, D.; Buckner, R.L.; Liu, H. Cerebellar asymmetry and its relation to cerebral asymmetry estimated by intrinsic functional connectivity. *J. Neurophysiol.* **2013**, *109*, 46–57. [[CrossRef](#)]
20. Kucyi, A.; Hodaie, M.; Davis, K.D. Lateralization in intrinsic functional connectivity of the temporoparietal junction with salience- and attention-related brain networks. *J. Neurophysiol.* **2012**, *108*, 3382–3392. [[CrossRef](#)]
21. Chiavaras, M.M.; Petrides, M. Orbitofrontal sulci of the human and macaque monkey brain. *J. Comp. Neurol.* **2000**, *19*, 35–54. [[CrossRef](#)]
22. Wosinski, M.; Schleicher, A.; Zilles, K. Quantitative analysis of gyrification of cerebral cortex in dogs. *Neurobiology* **1996**, *4*, 441–468. [[PubMed](#)]
23. Koyun, N.; Aydinlioğlu, A.; Aslan, K. A morphometric study on dog cerebellum. *Neurol. Res.* **2011**, *33*, 220–224. [[CrossRef](#)] [[PubMed](#)]
24. Sawada, K.; Horiuchi-Hirose, M.; Saito, S.; Aoki, I. Male prevalent enhancement of leftward asymmetric development of the cerebellar cortex in ferrets (*Mustela putorius*). *Laterality* **2015**, *20*, 723–737. [[CrossRef](#)] [[PubMed](#)]

Disclaimer/Publisher’s Note: The statements, opinions and data contained in all publications are solely those of the individual author(s) and contributor(s) and not of MDPI and/or the editor(s). MDPI and/or the editor(s) disclaim responsibility for any injury to people or property resulting from any ideas, methods, instructions or products referred to in the content.